Updated 21 cm Experiment Sensitivities

Jonathan Pober

ABSTRACT

This memo presents updated sensitivity calculations for various 21 cm experiments. Using the latest array models and an updated version of the 21cmSense code, these predictions should supersede those in the appendix of Pober et al. (2014).

1. Introduction

The appendix of Pober et al. (2014) contains a table of predicted sensitivities of various 21 cm instruments to the EoR power spectrum. The purpose of this memo is to update this table using (a) the latest version of the 21cmSense[1] code, which has seen several upgrades and additions, and (b) better or updated instrument models (e.g. the "re-baselined" SKA).

2. Observing Details

The 21cmSense code now supports both drift scans and tracked observing strategies. Sensitivities for both observing modes are presented for instruments with tracking capabilities. In the case of a drift scan, the observation assumes six hours of drift scanning data are taken over the same LST range each day for 180 days, for a total of 1080 hours of observation. For a tracked scan, the observation assumes two fields are each observed 3 hours a day over 180 days, for a total of 540 hours on each field. Other observing parameters (e.g. bandwidth, system temperature, etc.) are the same as used in Pober et al. (2014).

3. Foreground Models

In contrast with Pober et al. (2014), I have reduced the number of foreground models from three (formerly pessimistic, moderate, and optimistic) to two (now "avoidance" and "subtraction"). Both models now assume coherent addition of non-instantaneously redundant baselines (i.e. the pessimistic model has been discarded). Although the pessimistic model is representative of the PAPER analyses published to date, "partial redundancy" no longer seems viewed as a fundamental obstacle. The "foreground avoidance" and "foreground subtraction" models used here closely follow

[1] https://github.com/jpober/21cmSense

the moderate and optimistic models of Pober et al. (2014): a model where foregrounds contaminate all $k_{\|}$ modes $0.1h\mathrm{Mpc}^{-1}$ above the horizon limit, and a model where foreground contaminate only out to the first null of the primary beam[2], respectively.

4. $z = 9.5$ EoR Model

The reionization model used in Pober et al. (2014) comes from the default parameters of `21cmFAST` and reaches 50% ionization at $z = 9.5$. While the redshift of reionization is still quite uncertain, new measurements may hint that this redshift is pessimistically high (at least from the perspective of 21 cm experiments). I consider a new model which reionizes later in the section below; here in Table 1, I present sensitivities to the model used in Pober et al. (2014) to facilitate comparison. See Pober et al. (2014) for instrument descriptions.

Table 1: Sensitivities (i.e. "number of sigmas") of 21 cm EoR experiments to the reionization model used in Pober et al. (2014).

	Avoidance		Subtraction	
Instrument	Drift	Track	Drift	Track
PAPER 128	0.77	—	3.04	—
MWA 128	0.31	0.41	1.63	2.08
LOFAR	0.38	1.06	5.36	9.21
HERA 37	2.75	—	11.73	—
HERA 331	25.53	—	90.76	—
MWA 256[a]	1.02	1.24	5.54	6.51
SKA1 Low[b]	13.44	19.55	109.90	98.15

[a] The "Beardsley" proposed array. The final layout will likely move more antennas from the core to longer distances, reducing the EoR sensitivity of the instrument.

[b] Re-baselined design includes half the number of elements. Note that halving the number of stations removes the need for a redundant core, i.e., the desired SKA element density profile now can be achieved at all radii.

5. $z = 8$ Reionization Model

Recent measurements seem to hint at a lower redshift for 50% ionization than that used in the previous model, which was tuned in part to reproduce the WMAP optical depth. In this section, I present sensitivities for a new reionization history from `21cmFAST` which achieves 50% ionization at $z = 8$. I have also reduced the mean free path for ionizing photons through the IGM

[2] All beams in the sensitivity calculations are assumed to be Gaussian, but this "first null" corresponds to the angular distance from center were the beam an Airy disk.

in the simulation to values which may be more in line with recent observations (Andrei Mesinger, personal communication). This change lowers the amount of large scale 21 cm power, which does offset some of the sensitivity gain caused by the lower $T_{\rm sys}$ at lower z. The two reionization histories are compared in Figure 1. Table 2 gives the instrument sensitivities under this model.

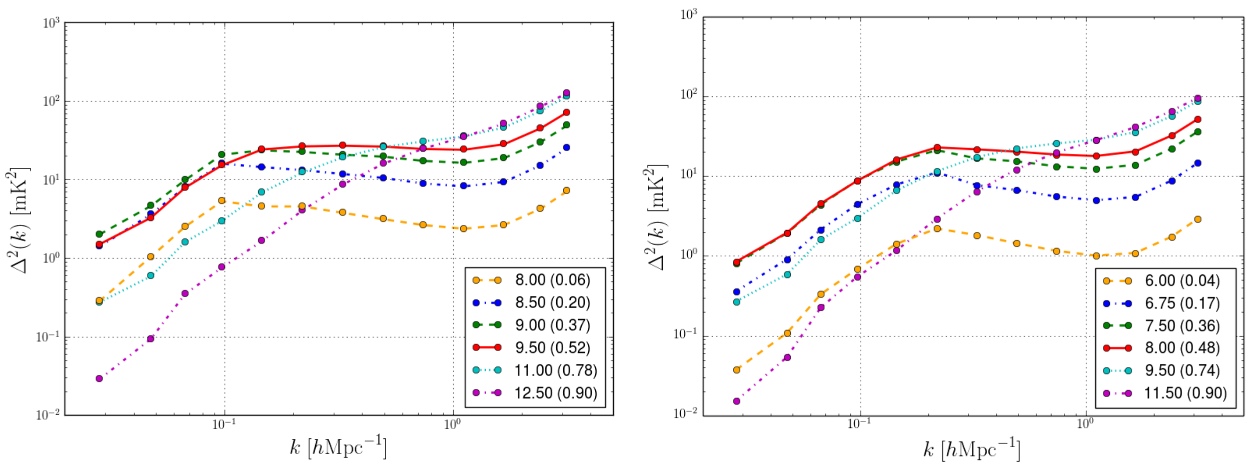

Fig. 1.— Left: the reionization model used in Pober et al. (2014) and §4. Right: the reionization model used here in §5. The legend lists the redshift of each power spectrum, with the corresponding neutral fraction in parenthesis.

6. Discussion

6.1. Comparison with Previous Calculations

The sensitivities reported here are somewhat different (generally more pessimistic) than those calculated in Pober et al. (2014); this results from changes in the public 21cmSense code compared with the code used in the paper. One major change is to force a strict relation between the dish/element effective area, the uv plane pixel size, the primary beam width, and the length of a coherent integration while in a drift scan mode. In the previous code, these quantities were all similar, but not actually forced to be directly related. Tied to this change is the move from the physical antenna area to an effective area, which has the most dramatic effect on wide-field arrays like PAPER and the MWA. Other changes come from the introduction of array layout changes (e.g. PAPER has moved from the theoretical 11×12 grid to the actually deployed 8×16 grid).

Comparing these results to the sensitivity predictions in Parsons et al. (2012) shows general consistency. Parsons et al. (2012) predicted a 3σ detection of a 30 mK^2 power spectrum using foreground avoidance and the same amount of observing time. I predict a 1.5σ detection of a ~ 20 mK^2 signal. Based on the decrease in power spectrum brightness alone, one would expect a

Table 2: Sensitivities (i.e. "number of sigmas") of 21 cm EoR experiments to a reionization model which achieves 50% ionization at a redshift of 8.

	Avoidance		Subtraction	
Instrument	Drift	Track	Drift	Track
PAPER 128	1.56	—	4.46	—
MWA 128	0.66	0.86	2.50	3.15
LOFAR	0.70	1.90	7.48	12.22
HERA 37	5.67	—	15.46	—
HERA 331	38.75	—	111.69	—
MWA 256[a]	2.40	2.81	8.28	9.64
SKA1 Low[b]	21.23	26.92	139.07	115.13

[a] The "Beardsley" proposed array. The final layout will likely move more antennas from the core to longer distances, reducing the EoR sensitivity of the instrument.

[b] Re-baselined design includes half the number of elements. Note that halving the number of stations removes the need for a redundant core, i.e., the desired SKA element density profile now can be achieved at all radii.

$\sim 2\sigma$ detection with our models. Parsons et al. (2012) also gain a $\sim 10\%$ sensitivity boost from logarithmic $|k|$ binning, and use 10% more observing time. Correcting for these factors, our results are quite consistent.

The results presented here for the MWA may seem more at odds with the calculation in Beardsley et al. (2013). Using a power spectrum model of comparable brightness to the one used here, and a foreground model nearly equivalent to our "subtraction" model, they predict a 14σ detection for 1600 hours of observation (split between two fields at 900 and 700 each). I predict a $\sim 3.2\sigma$ detection with 1080 hours of observing split evenly between two fields. Correcting for observing time, I would roughly expect a 50% decrease in sensitivity, yielding a 7σ detection. However, one major difference between these two calculations comes from the uv plane pixel size. To calculate overall sensitivities, both works assume every integration within a uv pixel adds coherently, whereas integrations on the same $|k|$ mode from different pixels add incoherently. Therefore, the result can be very sensitive to the choice of uv pixel size, which should coarsely represent the scale over which measurements can be considered redundant. As stated above, I use the effective area of the element to set the pixel size; for the MWA, this yields pixels of $(4.6\text{ m})^2$ at 150 MHz. Beardsley et al. (2013) use the instrumental window function from Bowman et al. (2006) to set a pixel size of $(8.3\text{ m})^2$. With a factor of 4 smaller pixel size, my calculation reduces the coherent integration by a factor of 4 while increasing the number of pixels by the same factor. Since separate pixels add incoherently, this results in a net loss of ~ 2 in sensitivity. Taking this factor into account, the results of the two calculations are in quite good agreement.

6.2. Sample Variance

It is interesting to note that for the arrays which can either drift or track, only the SKA gains from using a drift scan, and only in the foreground subtraction regime. This suggests that a long integration with the SKA will reach the sample variance limited regime, and covering additional sky area will be of benefit. (No attempt was made here to optimize the observing strategy, e.g., splitting the 1080 hours between three fields instead of two could yield higher significance measurements than the drift scan.)

6.3. North/South Baselines

For some time, I have argued the importance of North/South oriented baselines to these sensitivity calculations. Especially for arrays like HERA and PAPER, these baselines are short (high EoR sensitivity) and do not move in the *uv* plane (long coherent integration times). To date, we have not used these baselines in measurements with PAPER, since their slow fringe rate makes them very susceptible to cross-talk. In actuality, the sensitivity effect of removing these baselines is not terribly significant, causing only a $\sim 10\%$ decrease in sensitivity for the PAPER array and a $\sim 3\%$ decrease in sensitivity for HERA 331.

REFERENCES

Beardsley, A. P., et al. 2013, MNRAS, 429, L5

Bowman, J. D., Morales, M. F., & Hewitt, J. N. 2006, ApJ, 638, 20

Parsons, A., Pober, J., McQuinn, M., Jacobs, D., & Aguirre, J. 2012, ApJ, 753, 81

Pober, J. C., et al. 2014, ApJ, 782, 66

This preprint was prepared with the AAS LaTeX macros v5.2.